

## Improved Mechanical Performances of Triple Super Phosphate Treated Jute-Fabric Reinforced Polypropylene Composites Irradiated by Gamma Rays

M. Forhad Mina,<sup>1</sup> M. H. Shahid Shohrawardy,<sup>1,2</sup> Mubarak A. Khan,<sup>2</sup> A. K. M. Moshui Alam,<sup>2,3</sup> M. Dalour Hossen Beg<sup>3</sup>

<sup>1</sup>Department of Physics, Bangladesh University of Engineering and Technology, Dhaka-1000, Bangladesh

<sup>2</sup>Institute of Radiation and Polymer Technology, Bangladesh Atomic Energy Commission, Dhaka, Bangladesh

<sup>3</sup>Faculty of Chemical and Natural Resources Engineering, Universiti Malaysia Pahang, Gambang 26300, Kuantan, Malaysia

Correspondence to: M. F. Mina (E-mail: mfmna@phy.buet.ac.bd)

**ABSTRACT:** Untreated jute-fabric (JF) and triple-super-phosphate treated JF were incorporated in isotactic polypropylene (PP) to prepare sandwich composites. Untreated JF reinforced PP (UC) and treated JF reinforced PP composites (TC) were prepared using the compression molding technique at 180°C under a load of 5 tons. Both, TC and UC were irradiated by  $\gamma$ -rays at various doses to produce  $\gamma$ TC and  $\gamma$ UC. The highest tensile-strength (*TS*), flexural-strength (*FS*) and Young's modulus (*E*) were observed for the composite loaded with 55 wt % JF and irradiated at a dose of 5.0 kGy and. The maximum increases in *TS*, *FS*, and *E* of  $\gamma$ TC from UC are 17, 18, and 69%, whilst those of TC from UC are 12, 13, and 12%, respectively. Thermal degradation temperature of  $\gamma$ TC and TC is found to increase significantly from that of UC, suggesting an improved thermal stability of the treated composites. All these findings are explained on the basis of fiber-matrix interactions developed by the formation of physical and chemical bonds among JF and PP, as demonstrated by means of the Fourier transform infrared spectroscopy. © 2013 Wiley Periodicals, Inc. *J. Appl. Polym. Sci.* 130: 470–478, 2013

**KEYWORDS:** composites; fibers; mechanical properties; thermal properties; degradation

Received 8 November 2012; accepted 3 February 2013; published online 19 March 2013

DOI: 10.1002/app.39120

### INTRODUCTION

Natural fiber reinforced thermoplastics are considered as environmentally friendly candidates, which are being increasingly used as potentially ideal materials in automotive and construction industries.<sup>1,2</sup> Thermoplastic composites reinforced by natural fibers have gained much importance in automobile applications due to their high specific stiffness and specific strength as compared to conventional ones like aluminum and steel.<sup>3,4</sup> When natural fibers are introduced in polyolefin, the resulting materials achieve a high stiffness due to the robust elastic modulus of the individual single-fiber. Apart from these, natural fibers are advantageous over synthetic counterparts due to their low cost, low density, reduced energy consumption, carbon sequestration, recyclable nature, and above all biodegradability.<sup>5</sup>

Likewise other natural fiber, jute is a cheap and commercially available lignocellulosic fiber whose main component is cellulose,<sup>6</sup> which is basically a macromolecule consisting of anhydro-

D-glucose that contains hydroxyl (—OH) groups. These —OH groups make intramolecular and intermolecular hydrogen bonds inside the fiber and also make extramolecular bonds with the outside moist air. This tendency of forming extramolecular bond makes jute fiber hydrophilic in nature. The degree of hydrophilicity or the absorbance of moisture content by jute fiber can reach up to  $\approx 13\%$ .<sup>7</sup> Because of this moisture absorption, polymeric composites made of jute fiber and hydrophobic polymer result in poor mechanical strengths as compared to a pure polymer.<sup>8</sup> To overcome this drawback, fiber surface is usually treated by physical and chemical methods, which modify the surface structure and surface energy and make the fibers compatible with polymer matrix.<sup>9</sup> However, the survival of jute fiber in competition with its synthetic opponent depends on its cherished performances that are by far related to the shape, size, and surface texture of the fiber as well as its chemical structure. Under these circumstances, both surface and bulk status of jute fibers need to be modified by physical treatment, keeping their component structure almost unchanged so that they can be

aptly exploited. Jute fibers were reported to be exposed under high-energy gamma radiation ( $\gamma$ -ray) that has contributed not only to their physical and chemical changes in the bulk but also to the surface.<sup>10,11</sup> Several reports have documented improved performances of jute plastic composites.<sup>12–20</sup> Apart from these, a considerable number of investigations have been carried out by ionizing radiation technique, which has been popularly and successfully employed in crosslinking between cellulose fibers and polymers in the recently passed decades.<sup>6–8,10–14</sup> In ionizing radiation method,  $\gamma$ -ray interacts with solid cellulose by inelastic scattering, thereby creating trapped macrocellulosic radicals that are responsible for changing the physical, chemical and biological properties of cellulose fibers.

Conversely, isotactic polypropylene (PP) is a cheap, available and widely used semi crystalline thermoplastic polymer. It possesses valuable properties like transparency, high mechanical strength, high heat distortion temperature, low-moisture pickup, and good dielectric properties and has suitable filling, reinforcing and blending behavior with other polymers. Its fibrous nature creates a promising route to develop natural-synthetic polymer composites, alternatively called biodegradable plastics.<sup>21,22</sup> Considering their cost effectiveness, availability and other valued properties, jute fiber and PP can respectively be preferable natural fibers and a thermoplastic polymer to tailor eco-friendly, biodegradable plastic composite with desirable properties. Conversely, treated natural fiber reinforced polymeric composites usually showed better mechanical performances than untreated fiber based composites.<sup>9</sup> Therefore, it is necessary to find out a suitable treatment route that is economically viable as compared to the traditional treatment methods. Based on this notion, the present work has been undertaken to treat jute fabric by triple super phosphate (TSP), which is a cheap and an extensively used fertilizer in agriculture. Furthermore, if the chemically treated jute fiber is added to PP for production of biodegradable composite, which is then irradiated by  $\gamma$ -rays, then a significant change in materials properties of the composite can be expected. Thus, one of the objectives of this work is to treat jute fiber by TSP and the other aim is to irradiate both the untreated and treated jute fabric composites with varying  $\gamma$ -ray doses for changing their materials' performances. Then, comparisons of the changes in structural, mechanical, and thermal properties of the resulting  $\gamma$ -ray irradiated composites with respect to the nonirradiated ones have been done, and the results obtained are elaborately discussed in this study.

## EXPERIMENTAL

### Sample Preparation

Jute fabric (JF) (commercial grade), a woven mat of jute fiber, were supplied from Bangladesh Jute Research Institute, Dhaka, Bangladesh and PP was purchased from Polyolefin Company, Singapore. To chemically treat the original or untreated JF, it was soaked in TSP solution ( $\approx 15\%$ , w/v) kept in a mechanical shaker, shaken for about 20 min and then dried in an oven at  $100^\circ\text{C}$ . The TSP fertilizer of chemical formula  $3\text{Ca}(\text{H}_2\text{PO}_4)_2$  was obtained from Bangladesh Chemical Industries Corporation, Bangladesh. The TSP-treated JF was cut into a size of 15-cm long and 12-cm wide. Polymer sheets of average thickness

$\approx 0.25$  mm were prepared from granules of PP by pressing at  $180^\circ\text{C}$  between two steel molds under a load of 5 tons using a heat-press machine (Carver with hydraulic unit model-3925, Carver INC., Indiana, USA). The thickness of JF was in the range  $\approx 0.50$ – $0.60$  mm. Both PP sheet and JF were cut into the same size (length  $\times$  width) of the mold (ASTM-D638-V). The fabric reinforced PP composites were fabricated by pressing a sandwich of four layers of JF in between five layers of pre-weighed PP sheets using compression molding technique at  $190^\circ\text{C}$  under a 5 tons load for 30 min to allow molten PP to be diffused in JF layers and cooled to room temperature in an ambient condition. The weight ratios of JF contents were maintained approximately as 35, 40, 45, 50, 55, and 60 wt % by changing the weight of the PP sheets. Thus, the sample thickness varies as according to the fiber content in it.

The samples prepared with JF contents greater than 60 wt % consisted of lack of homogeneity and were, therefore, discarded for further investigation. The untreated JF-reinforced PP composites and TSP-treated JF reinforced PP composites are hereinafter abbreviated as UC and TC, respectively. Both these composites were subjected to mechanical tests to optimize the JF content. After testing, the composites that exhibited the highest tensile/flexural strength were considered as the optimized fiber system for further experimental study. Then, the UC and TC after exposing to  $\gamma$ -rays by a Cobalt-60 irradiator (62 kCi, Brit, India) are labeled as  $\gamma$ UC and  $\gamma$ TC, respectively. For exposing the samples under  $\gamma$ -rays, three different doses of 2.5, 5.0 and 7.5 kGy, were used, maintaining a rate 3.5 kGy/h. The dose was determined by a Fricke dosimeter, which was an aerated solution of ferrous sulfate ( $\text{FeSO}_4$ ) in aqueous sulfuric acid ( $\text{H}_2\text{SO}_4$ ) solution. The solution was simultaneously irradiated with the samples. The original ferrous sulfate was colorless and became colored ferric sulfate after irradiation. Measuring the optical density of the irradiated solution by a spectrophotometer, the amount of doses was evaluated. All the samples fabricated were then investigated by the following experimental methods.

### Fourier-Transforms Infrared Spectroscopy

Fourier-transform infrared (FTIR) spectra of the samples were recorded at room temperature by using a double beam FTIR spectrophotometer (SHIMADZU, FTIR 8900 spectrophotometer, Japan) in the wavenumber range of  $500$ – $4000$   $\text{cm}^{-1}$ . For these measurements, the samples were crashed by a plastic crusher. During crashing, a small amount of powder form of each sample was obtained. This powder was mixed thoroughly with pure potassium bromide (KBr) and the mixture was then compressed in a metal holder under a load of 8–10 tons to produce a pellet for recording the FTIR spectrum in the transmittance (%) mode.

### Mechanical Test

Tensile and bending properties of PP and composites were studied using a universal testing machine (model 1011, UK). Tensile strength ( $TS$ ) and Young's modulus ( $E$ ) of PP, JF and various composites were measured with a crosshead speed of 10 mm/min and a gauge length of 20 mm. The load was continuously applied to the sample till it is fractured. Bending or flexural strength ( $FS$ ) of these samples was also measured by a

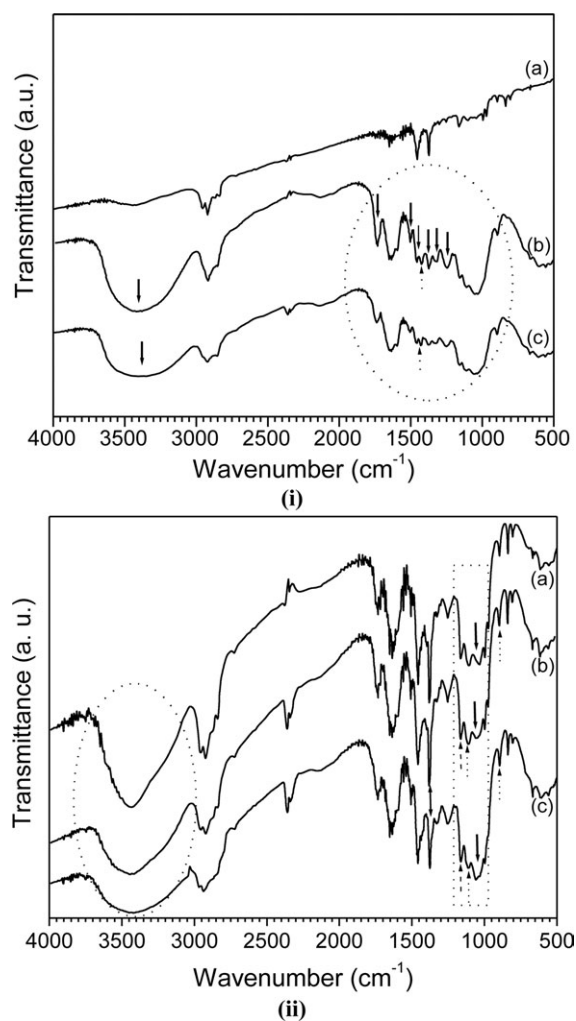


**Figure 1.** FTIR spectra for (i) PP (a), untreated JF (b) and treated JF (c) as well as for (ii) UC (a), TC (b) and  $\gamma$ TC at 5.0 kGy (JF content in the composites is 55 wt %).

three-point bending test with a loading speed of 2 mm/min and a supporting span of 36 mm. Five samples from PP and composites of each JF content were subjected to mechanical measurements according to ASTM standards.

### Surface Morphology

Surface morphology of the fractured surface of the samples was studied by the scanning electron microscopy (SEM) [ZEISS, EVO50, Philips XL30, Netherlands] with a maximum operating voltage of 30 kV of the apparatus. Surface micrographs were taken at a magnification of 100 $\times$  or with a scale of 200  $\mu$ m. Samples of suitable size were prepared first and attached appropriately on the sample holder. The sample surface was coated with a thin gold layer by a sputtering machine prior to SEM measurements.

### Thermal Measurements

Thermal properties of the samples were monitored by a coupled differential thermal analyzer (DTA) and thermogravimetric analyzer (TGA) [Seiko-Ex-STAR-6300, Japan]. The measurements using DTA and TGA were carried out from room temperature

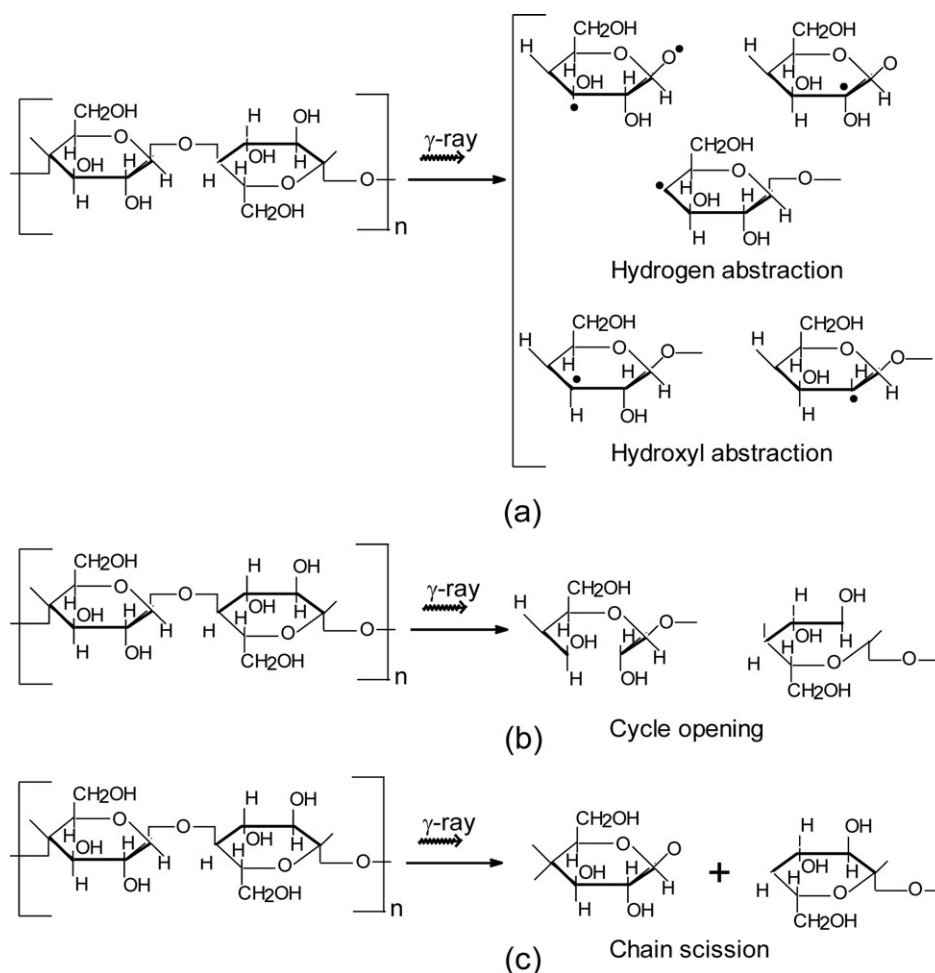
(37 $^{\circ}$ C) to 600 $^{\circ}$ C at a heating rate of 20 $^{\circ}$ C/min under nitrogen gas flow. The DTA traces provide the melting and degradation temperatures of the samples as determined from the exotherm versus temperature curves and the TGA runs exhibit the weight-loss of the sample with temperature. All these information were monitored and analyzed by DTA.

## RESULTS AND DISCUSSION

### Structural Analyses from FTIR Spectra

Figure 1(i) shows the FTIR spectra for PP, untreated JF and TSP-treated JF in the same scale-range of transmittance (a.u.) for all samples to compare the peak intensity. Several peaks of the spectrum of PP [Figure 1(i-a)] coincide with the reported values that were attributed to microstructures of crystalline, paracrystalline and amorphous phases of PP by other researchers.<sup>21</sup> These authors assigned the vibrational modes to the low wavenumber range (<1165 cm<sup>-1</sup>) as the C—C stretching mode of backbone orientation. The spectrum of untreated JF [Figure 1(i-b)] shows absorption bands of cellulose, hemicellulose and lignin, which are originated from alkenes as well as aromatic and different oxygen containing functional groups of ester, ketone, and alcohol. The important absorption bands for untreated JF, as indicated by arrows, are located at 3200–3600 cm<sup>-1</sup> for the stretching vibration of hydrogen bonded O—H groups. The other important absorption bands appear at 1738 cm<sup>-1</sup> for the C=O stretching vibration of the carboxyl and ester groups in hemicellulose, whilst those are at 1500 cm<sup>-1</sup> for the CH<sub>2</sub> deformation, 1452 cm<sup>-1</sup> for the CH<sub>3</sub> asymmetric deformation, 1370 cm<sup>-1</sup> for the CH symmetric deformation, 1030 cm<sup>-1</sup> for the CH in-plane deformation and 1235 cm<sup>-1</sup> for the C—O—C stretching vibration of acetyl groups in lignin,<sup>22,23</sup> as indicated inside the dotted enclosure. In contrast, the peak at 1430 cm<sup>-1</sup> (upward arrow) for the CH<sub>2</sub> bending of cellulose remains almost unaffected after treatment.<sup>23</sup> All these peaks, which are noticeable with a reduced intensity in the spectrum of TJF, demonstrate a partial removal of hemicellulose and lignin, pectin etc. from JF by TSP treatment. Similar removal of non-cellulosic components from natural fibers by alkaline treatment has been reported elsewhere.<sup>16,17,24</sup>

Figure 1(ii) shows the FTIR spectra of UC, TC and  $\gamma$ TC of a dose 5.0 kGy (JF = 55 wt %). The most conspicuous changes in the spectra are found in the wavenumber ranges of 3200–3600 cm<sup>-1</sup> and 1000–1200 cm<sup>-1</sup>, as bounded by dotted enclosures. The C—O vibrations of crystalline and amorphous cellulose in both the spectra of UC and TC [Figure 1(ii-a,b)] similarly appear at 1113 and 910 cm<sup>-1</sup> (upward dotted arrows), respectively.<sup>21,24</sup> In contrast, the spectrum of  $\gamma$ TC [Figure 1(ii-c)] indicates a reduction in intensity of C—O vibrations from crystalline part that proves a breaking of crystalline cellulose by  $\gamma$ -ray irradiation. Moreover, an increase in intensity of 1162 cm<sup>-1</sup> (upward dashed arrows) band, which is related to the antisymmetric stretching of C—O—C glycoside bonds, may indicate the formation of this bond with PP molecules. Besides, changes in intensity of C—O stretching (at 910 cm<sup>-1</sup>) of amorphous cellulose and that of hydrogen bonded O—H stretching are also noticeable. Moreover, C—H stretching of cellulose at 1375 cm<sup>-1</sup> is found to be notably changed after  $\gamma$ -ray



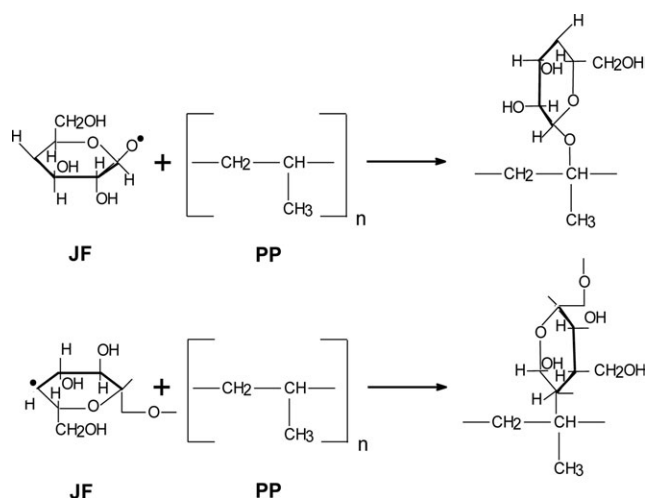
**Scheme 1.** (a) Hydrogen and hydroxyl abstraction, (b) cycle opening and (c) chain scission mechanisms of cellulose molecules in JF after  $\gamma$ -ray irradiation.

irradiation. To explain these results, we invoke the crosslinking mechanism between JF and PP molecules by ionizing radiation process, as proposed earlier.<sup>25</sup> Notably, no FTIR spectroscopic results were provided to demonstrate the previously proposed cross-linking mechanism. Therefore, a part of this mechanism has been newly delineated in Schemes 1 and 2 to correlate the crosslinking phenomena with the FTIR spectral findings. According to this mechanism, free radicals (as marked by small black circles) are formed after C–H, C–O, and C–C bond cleavages of the monomeric units of  $\beta$ -D-glucopyranose of jute through hydrogen and hydroxyl abstraction (a), cycle opening (b) and chain scission (c) by  $\gamma$ -radiation (Scheme 1). Thereafter, JF and PP molecules join together through the C–C and C–O–C bonds (Scheme 2). The observed increase in C–O–C bond intensity confirms the formation of this bond, whereas the intensity increase at the downward solid arrow ( $\sim 1050\text{ cm}^{-1}$ ) may indicate the C–C stretching mode of the JF-PP link. Thus, the observed findings of FTIR spectra corroborate the proposed crosslinking mechanism between cellulose and PP.

### Mechanical Properties

The change in *TS*, *FS*, and *E* from 35 to 60 wt % JF contents for UC and TC are shown in Figure 2(i–iii), respectively. The

highest *TS* values of 52 and 58 MPa, *FS* values of 53 and 59 MPa and *E* values of 420 and 472 MPa are found for UC and TC at 55 wt % JF content, respectively. The *TS*, *FS*, and *E* increases of TC from UC after TSP treatment of fabric are



**Scheme 2.** The crosslinking mechanism between the cellulose and PP molecules.

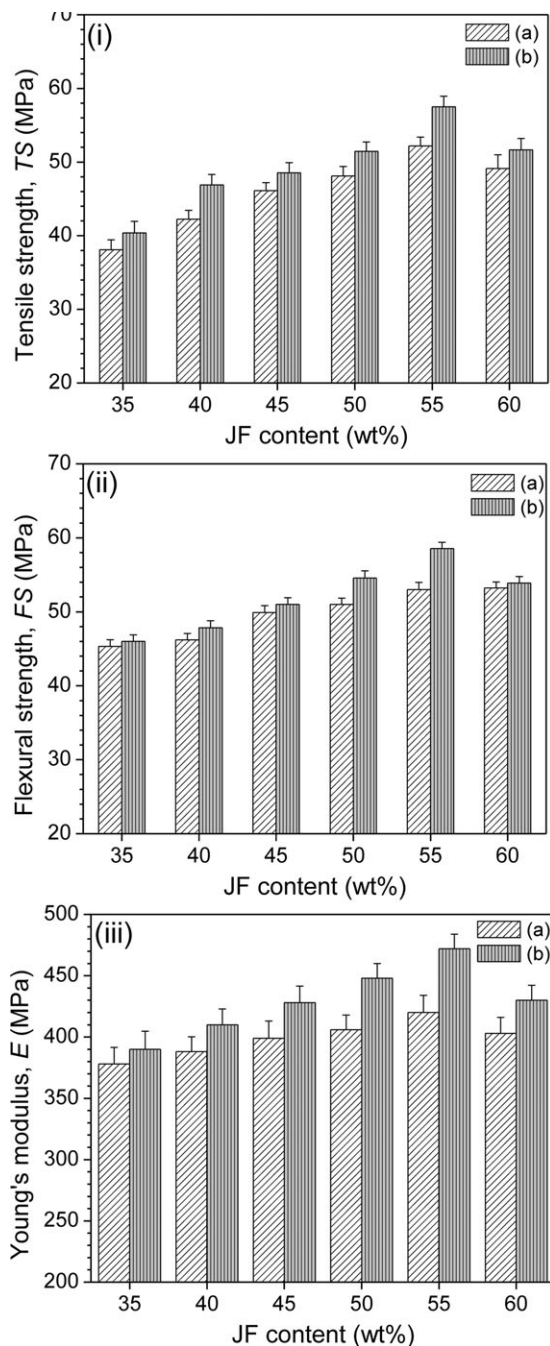


**Figure 2.** The changes in (i)  $TS$ , (ii)  $FS$  and (iii)  $E$  with respect to JF content for UC (a) and TC (b).

about 12, 13, and 12%, respectively. Besides, increasing fabric content increases the mechanical properties and nearly 55 wt % JF content in PP produces a relatively strong composite of PP and jute fabric. As the  $TS$  and  $E$  of JF is lower than that of PP,<sup>25,26</sup> it is rational to expect the mechanical properties of the composites in between those of PP and JF. Nevertheless, the increase of JF content in composites unexpectedly increases the  $TS$ , and an optimal adhesion between PP and JF can be suggested from the highest mechanical performances of the composites occurring at 55 wt % JF content. Moreover, the higher  $TS$ ,

$FS$ , and  $E$  values of TC than UC at any loading of JF indicate that TSP treatment provides better performance of the resulting composites. Figures 3(i–iii) respectively illustrate the  $TS$ ,  $FS$ , and  $E$  versus  $\gamma$ -ray dose plots for  $\gamma$ UC and  $\gamma$ TC, which contain 55 wt % JF content. Clearly, an increase in mechanical properties with the increase in  $\gamma$ -ray dose up to 5 kGy is observed, and after that the mechanical properties decreases. For  $\gamma$ UC and  $\gamma$ TC the observed maximum  $TS$  values are 58 and 61 MPa,  $FS$  values 61 and 63 MPa and  $E$  values 650 and 710 MPa, respectively. Thus, the  $TS$ ,  $FS$ , and  $E$  increases of  $\gamma$ TC at a dose of 5.0 kGy from the maximum  $TS$  values of UC are 17, 18, and 69%, respectively. Conversely, these increases of  $\gamma$ UC from UC are about 12, 7, and 55%, respectively. These results demonstrate a

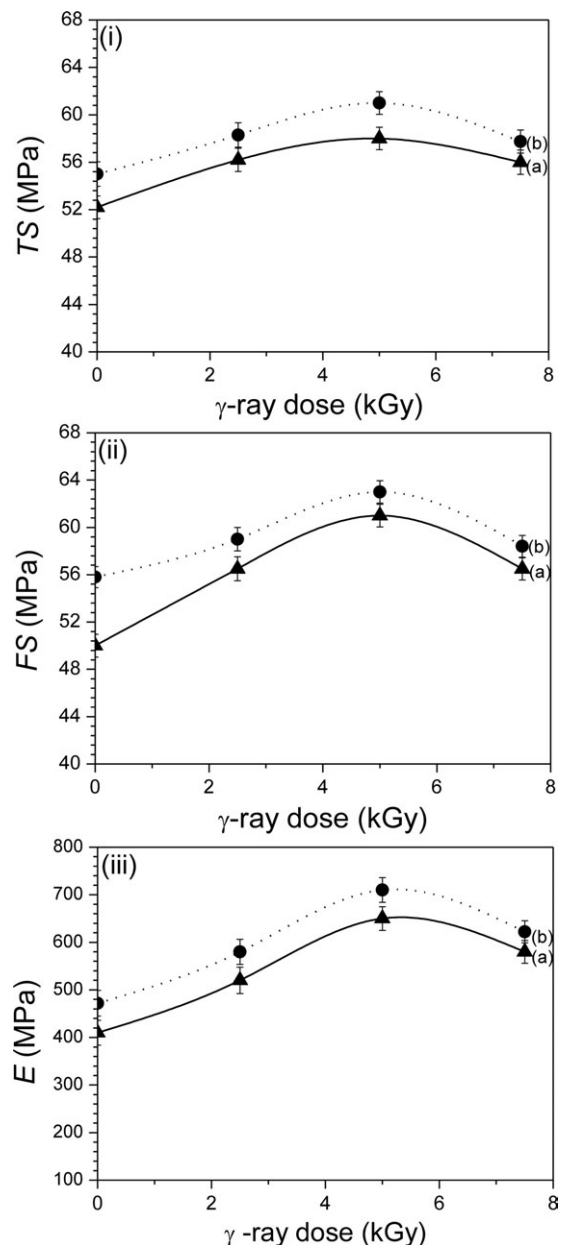


**Figure 3.** The variations in (i)  $TS$ , (ii)  $FS$  and (iii)  $E$  with respect to  $\gamma$ -ray dose for (a) UC and (b) TC having 55 wt % JF content.

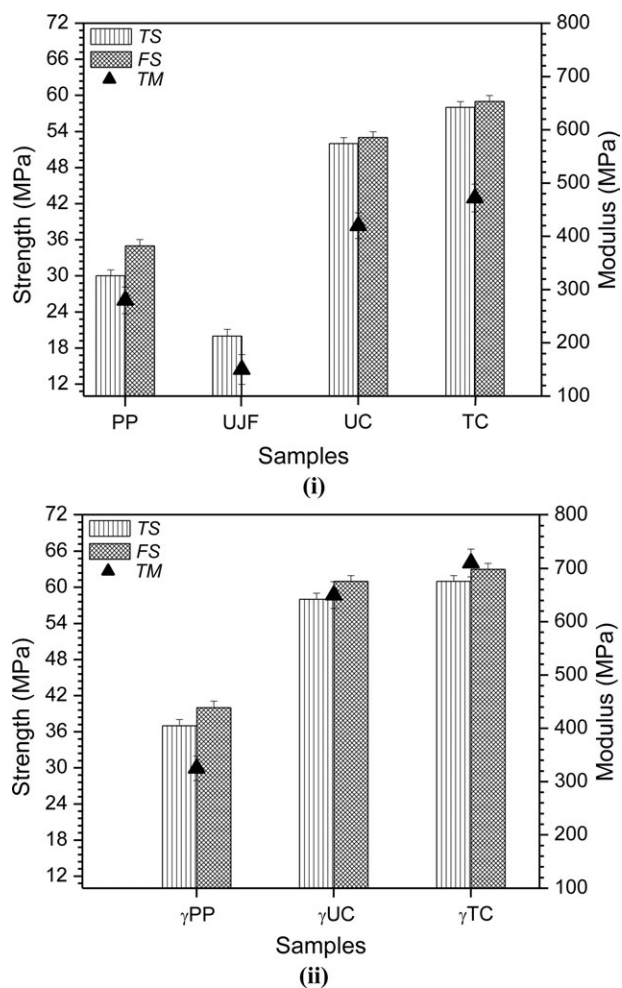


**Figure 4.** Comparisons of the maximum mechanical properties (*TS*, *FS* and *E* values) for samples prepared (i) without  $\gamma$ -ray irradiation and (ii) with  $\gamma$ -ray irradiation at the dose of 5.0 kGy. The *TS* and *FS* are represented by the left vertical scale.

significant increase in Young's modulus and a considerable increase in strengths of the composites after  $\gamma$ -ray irradiation. A comparison of the maximum *TS*, *FS*, and *E* values for different samples are presented in Figure 4(i,ii), wherein  $\gamma$ TC shows the highest values of mechanical properties among all others.

The increase in *TS* and *E* of the composites due to the inclusion or increase of untreated JF content may be attributed to the fact that instead of jute-fabrics individual jute fibers are apparently contributing to the ultimate increase in mechanical properties because their robust *TS* value of 393–773 MPa and *E* value of 13–27 GPa.<sup>26</sup> However, when JF content is greater than 55 wt %, the composites become inhomogeneous because of the fiber–fiber interaction whose effect may cause to develop voids or fiber-agglomeration in the composites and thus results in lowering the *TS* and *E* values. Effects of TSP treatment and  $\gamma$ -ray irradiation on mechanical properties of the composites occur due to the formation of chemical and physical bonds, which are evidenced from the FTIR spectral changes of  $\gamma$  TC and TC from UC. The increase in mechanical properties of TC from UC may be attributed to the elimination of the oily and

gluey components from JF by TSP treatment. This removal of waxy components makes the fabric surface rough, thereby increasing the van der Waals interaction between molecules of PP and fabric. Enhancement in mechanical properties of composites after  $\gamma$ -ray treatment may be attributed to the development of crosslinking between PP-PP molecules, JF-JF molecules, and PP-JF molecules. In the early reported crosslinking mechanism, the authors claimed that the increase in *TS* is due to the increased density of molecular crosslinking, which depends on the  $\gamma$ -ray dose.<sup>25</sup> Our observed FTIR spectral changes also conform to this claim. However, the *TS* decrease after 5.0 kGy can be due to the breaking of long chain bonds of PP and various molecules of JF, as discussed earlier.

### Surface Morphology

Figure 5(a,b) represent SEM micrographs of the fractured surface of UC and TC prepared with 55 wt % JF. Figure 4(c,d) shows the fractured surface micrographs of  $\gamma$ TC with 55 wt % JF content for doses of 5.0 and 7.5 kGy, respectively. When the composites are deformed by tensile measurements, the fabrics get stretched. With increasing applied load, the fabrics can be detached from the PP matrix, and the degree of detachment depends on their adhesion with matrix. After fracturing the samples by deformation, the fibers are either torn or pulled out randomly from PP matrix. Jute fibers are clearly seen on each micrograph where UC shows more fibers pull-out than TC. This implies that a better adhesion between JM and PP is observed by TSP treatment. Despite this, the adhesion between JM and PP is not homogeneous everywhere in the sample. Therefore, the location of poor contact between JM and PP get easily separated, and the fibers can come out from the PP matrix. Conversely, micrographs of all  $\gamma$ -ray irradiated samples indicate comparatively smoother surfaces than those of UC and TC, and a few fibers are pulled out from the matrix. The observed micrographs suggest that the interaction between JM and PP has notably been increased by both TSP and  $\gamma$ -ray treatments.

### Thermal Properties

The DTA thermograms of PP and other samples are presented in Figure 6. Each thermogram contains several peaks that correspond to melting temperature ( $T_m$ ) of the solid sample and degradation temperature ( $T_d$ ) of the molecules of this solid. The peak temperature of each thermogram is compared by the lines L1, L2, and L3. The DTA run of PP [Figure 6(a)] contains two peaks that represent a sharp melting temperature ( $T_m^{PP}$ ) at 167°C and a sharp degradation temperature ( $T_d^{PP}$ ) at 450°C of PP. The untreated JF shows a diffuse peak at 85°C (as indicated by an arrow), which can be defined as the temperature  $T_d^{H_2O}$  at which the absorbed water starts to emit from the fabric. The untreated JF also shows a sharp endothermic peak at 369°C, indicating the degradation temperature  $T_d^{JF}$  of some of its components [Figure 6(b)]. A small downward fall nearly at 300°C, as indicated by the double-arrow, may be associated with the decomposition of hemicellulose from JF.<sup>27,28</sup> Conversely, all composites clearly reveal four endothermic peaks [Figure 6(c–e)]. The peak at 85°C can be assigned to the release of water molecules from the fabric, which has been also reported by others.<sup>29</sup> The peak at 167°C can be attributed to the dissociation of PP

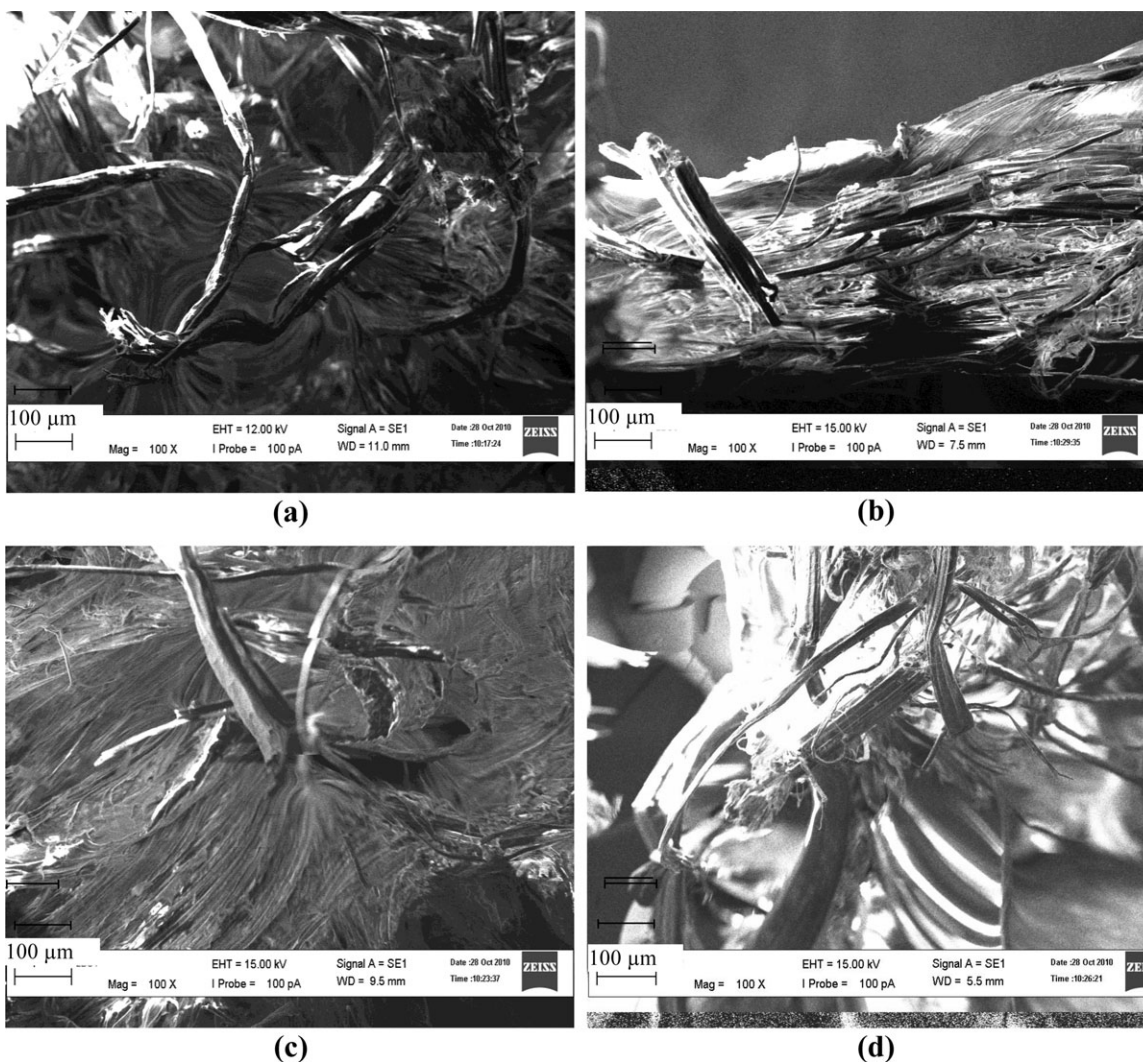


**Figure 5.** SEM micrographs of the fractured surface of composites with 55 wt % JF content: (a) UC, (b) TC, (c)  $\gamma$ TC at 5.0 kGy and (d)  $\gamma$ TC at 7.5 kGy.

molecules. The peaks at 369 and 450°C represent the degradation temperatures of molecules of PP and JF, respectively. The most striking observations found here are the disappearance of the  $T_d^{H_2O}$ -peak and a slight shift of all peaks. The melting temperature of composites is found to be lower than that of PP. This result may be associated with the disordered crystalline structures possibly developed in the lamellae of PP and the cellulose of JF during fabrication. The melting temperature of  $\gamma$ TC slightly increases with increasing  $\gamma$ -ray doses (Figure 7). This increase is possibly related to the breaking of chemical and adhesive bonds, whose formation by  $\gamma$ -rays has been suggested and discussed earlier.

The TGA runs shown in Figure 8(i-a-e) exhibit the weight loss with increasing temperature for PP, untreated JF, UC, TC and  $\gamma$ TC, respectively. The thermal degradation of neat PP takes place in one step in which the onset of weight-loss occurs at 380°C and finishes at 480°C. This degradation was ascribed by the dissociation of C—C chain bonds along with H-abstraction at the site of dissociation.<sup>28,30</sup> The cleavage of PP chain

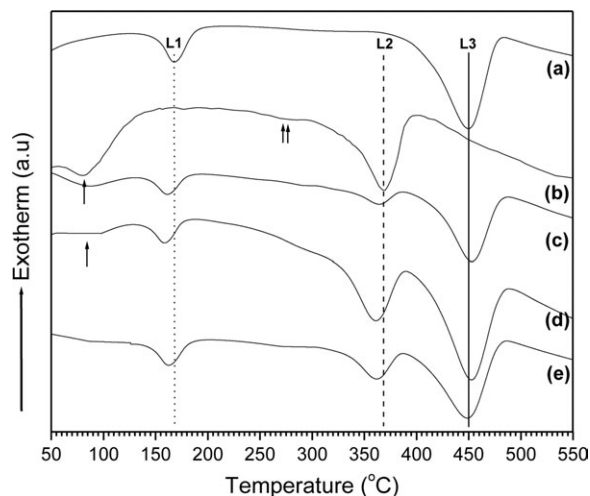


**Figure 6.** DTA thermograms for (a) PP, (b) untreated JF, (c) UC, (d) TC and (e)  $\gamma$ TC at a dose of 5.0 kGy (JF content in composites is 55 wt %).

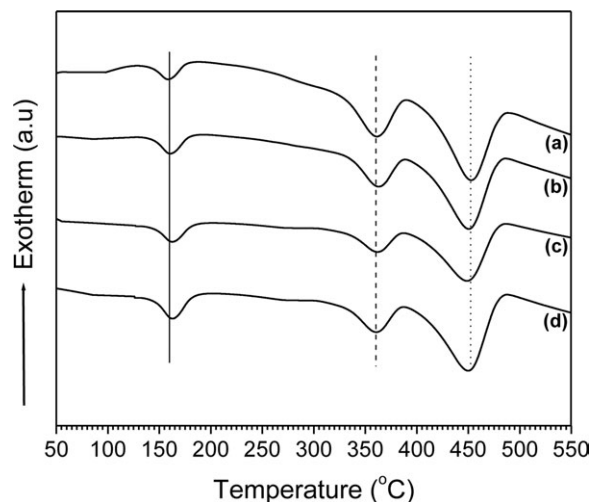


**Figure 7.** DTA thermograms for  $\gamma$ TC prepared with 55 wt % JF content at doses of 0 (a), 2.5 (b), 5.0 (c) and 7.5 (d) kGy.

molecules was reported to occur at the bonds adjacent to the weakest tertiary carbons bond.<sup>31–33</sup> The degradation of JF shows a two-step process. It commences at 85°C (as indicated by the arrow) due to water release, accompanied by a sharp fall at 250°C and ends at 380°C. According to a previous publication,<sup>30</sup> untreated natural fibers were shown to suffer thermal degradation in a two-stage process of which the first part occurred in the temperature range 200–310°C and the second part in the range 310–400°C. Our results are in agreement with these findings. Contrary to these, JF based PP composites exhibit a three-step degradation process. An indicator commonly practiced to characterize the structural degradation or destabilization is to consider the  $T_d$  at 50% weight loss of a sample.<sup>34</sup> The  $T_d$  values thus evaluated from the TGA curves for various samples are introduced in Table I. Analysis shows that the  $T_d$  increases for TC and  $\gamma$ TC from UC are 17 and 21°C, respectively. This increase demonstrates the formation of physical and chemical bonds among JF and PP molecules by surface treatment and  $\gamma$ -ray irradiation, respectively. The TGA runs for  $\gamma$ TC at  $\gamma$ -ray doses of 2.5 and 7.5 kGy are illustrated in Figure 8(ii).

**Table I.** Degradation Temperatures Obtained for Different Samples, as Evaluated from 50% Weight Loss from the TGA Thermograms

| Samples ID   | Processing conditions |                          | Value at 50% weight loss $T_d$ (°C) |
|--------------|-----------------------|--------------------------|-------------------------------------|
|              | JF content (wt %)     | $\gamma$ -ray dose (kGy) |                                     |
| PP           | 0                     | 0                        | 449                                 |
| Untreated JF | 100                   | 0                        | 350                                 |
| UC           | 55                    | 0                        | 410                                 |
| TC           | 55                    | 0                        | 427                                 |
| $\gamma$ TC  | 55                    | 2.5                      | 429                                 |
|              | 55                    | 5.0                      | 431                                 |
|              | 55                    | 7.5                      | 416                                 |

The  $T_d$  values of these samples are also tabulated (Table I). The low  $T_d$  value of the composite irradiated with higher dose can suggest the degradation of the molecules of PP and JF.

The onset temperature of degradation for UC, TC, and  $\gamma$ TC at 300°C may be referred to the decomposition of hemicellulose.<sup>27,28</sup> The middle stage degradation of TGA (Figure 8) may be attributed to the decomposition of  $\alpha$ -cellulose and lignin.<sup>28</sup> These results are in concurrent with those published in an article, wherein the authors have declared a lower thermal stability in the wood floor-based PP composites due to lower thermally stable wood floor.<sup>27</sup> More interestingly, the weight loss pattern for the  $\gamma$ -ray treated composites is unlike that of other samples, immediately after the rapid weight-loss. The mechanism of this disintegration also gives us a sign of the bond formation in the composites due to  $\gamma$ -ray irradiation. The low temperature degradation process is associated with degradation of hemicellulose, whereas the high temperature process corresponds to the degradation of cellulose and is also associated to the pyrolysis of lignin involving fragmentation of interunit linkages (releasing monomeric phenols into the vapor phase), decomposition, and

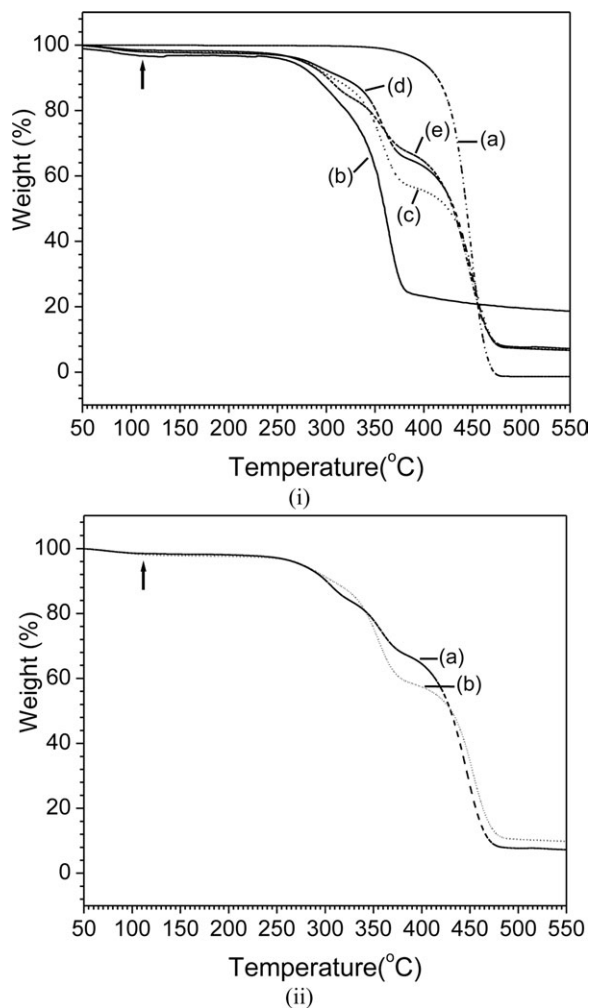


**Figure 8.** TGA runs of (i) PP (a), untreated JF (b), UC (c), TC (d) and  $\gamma$ TC at a dose of 5.0 kGy as well as of (ii)  $\gamma$ TC at 2.5 (a) and 7.5 (b) kGy (JF content in composites is 55 wt %).



condensation of the aromatic rings.<sup>31,32</sup> The formation of char residues may involve initial physical desorption of water, intramolecular dehydration, formation of carboxyl and carbon-carbon double bonds, cleavage of glycosidic linkage and rupture of C—O and C—C bonds and condensation and aromatization of carbon atoms from each original pyranose ring to form discrete graphite layers, as declared elsewhere.<sup>16,33</sup>

## CONCLUSIONS

JF reinforced PP composites have been fabricated with various contents of untreated and TSP treated JF. These composites have then been irradiated by  $\gamma$ -ray, which causes to develop chemical bonding that have sufficiently influenced on their mechanical, surface morphological, and thermal properties. The FTIR spectra make it confirmed the formation of new bonds in the composites by both chemical and physical treatments. A considerable increase in mechanical properties like *TS*, *FS*, and *E* is observed for  $\gamma$ TC from TC, whereas a moderate increase of these properties for TC from UC is found, suggesting better mechanical performances of the composites treated by  $\gamma$ -rays and fibers treated by TSP. A better adhesion between JF and PP is clearly noticeable by SEM observations. The  $\gamma$ TC and TC are found to degrade at an elevated temperature of about 20°C from 410°C shown by UC as evaluated by TGA, indicating the treated composites to be thermally more stable than the untreated ones. A coherence of the results from all observations is observed.

## ACKNOWLEDGMENTS

The authors greatly acknowledge the Bangladesh University of Engineering and Technology (BUET) to provide financial support for this investigation. They are grateful to the Atomic Energy Research Establishment (AERE), Bangladesh Council of Scientific & Industrial Research (BCSIR) and Universiti Malaysia Pahang to allow facilities for this research.

## REFERENCES

- Malkapuram, R.; Kumar, V.; Yuvraj, S. N. *J. Reinf. Plast. Compos.* **2008**, *28*, 1169.
- Wambua, P.; Ivens, J.; Verpoest, I. *Compos. Sci. Technol.* **2003**, *63*, 1259.
- Holbery, J.; Houston, D. J. *Miner. Met. Mater. Soc.* **2006**, *58*, 80.
- Albrecht, N.; Becker, U.; Thoma, W. *J. Polym. Environ.* **2002**, *10*, 115.
- Ku, H.; Wang, H.; Pattarachaiyakoop, N.; Trada, M. *Compos. Part B Eng.* **2011**, *42*, 856.
- Hassan, M. M.; Islam, M. R.; Shehzade, S.; Khan, M. A. *Polym. Plast. Technol. Eng.* **2003**, *42*, 515.
- Khan, M. A.; Haque, N.; Kafi, A. A.; Alam, M. N.; Abedin, M. Z. *Polym. Plast. Technol. Eng.* **2006**, *45*, 607.
- Hassan, M. M.; Khan, M. A.; Islam, M. R. *Polym. Plast. Technol. Eng.* **2005**, *44*, 833.
- Vilaseca, F.; Llop, M.; Gironès, J. Méndez, J. A.; Mutjè, P. *J. Hazard Mater.* **2007**, *144*, 730.
- Haydar, U. Z.; Khan, A. H.; Hossain, M. A.; Khan, M. A.; Khan, R. *Polym. Plast. Technol. Eng.* **2009**, *48*, 760.
- Khan, M. A.; Khan, R. A.; Haydar, U. Z.; Hossain, A.; Khan, A. H. *J. Reinf. Plast. Compos.* **2013**, *28*, 1651.
- Khan, M. A.; Hinrichsen, G.; Drzal, L. T. *J. Mater. Sci. Lett.* **2001**, *20*, 1711.
- Haydar, U. Z.; Khan, A. H.; Hossain, M. A.; Khan, M. A.; Khan, R. *Polym. Plast. Technol. Eng.* **2009**, *48*, 760.
- Khan, M. A.; Hassan, M. M.; Drzal, L. T. *Compos. Part A Appl. Sci. Manuf.* **2005**, *36*, 71.
- Mohanty, A. K.; Khan, M. A.; Hinrichsen, G. *Compos. Sci. Technol.* **2000**, *60*, 1115.
- Jahangir, A.; Khan, M. A.; Khan, R. I.; Gafur, A. *Mater. Sci. Appl.* **2010**, *1*, 350.
- Yang, Y.; Ota, T.; Morii, T.; Hamada, H. *J. Mater. Sci.* **2011**, *46*, 2678.
- Acha, B. A.; Marcovich, N. E.; Reboledo, M. M. *J. Appl. Polym. Sci.* **2005**, *98*, 639.
- Karmaker, A. C.; Youngquist, J. A. *J. Appl. Polym. Sci.* **1996**, *62*, 1147.
- Van Den Oever, M. J. A.; Snijder, M. H. B. *J. Appl. Polym. Sci.* **2008**, *110*, 1009.
- Park, D. K.; Park, J. W.; Kim, I.; Ha, C. S. *J. Adhes. Int.* **2005**, *6*, 1.
- Liu, X. Y.; Dai, G. C. *Express Polym. Lett.* **2007**, *1*, 299.
- Morshed, M. M.; Alam, M. M.; Daniels, S. M. *Plasma Sci. Technol.* **2010**, *12*, 325.
- Alam, A. K. M. M.; Beg, M. D. H.; Prasad, D. M. R.; Khan, M. R.; Mina, M. F. *Compos. Part A Appl. Sci. Manuf.* **2012**, *43*, 1921.
- Haydar, U. Z.; Khan, R. A.; Mubarak, A. K.; Khan, H.; Hossain, M. A. *Radiat. Phys. Chem.* **2009**, *78*, 986.
- Saha, P.; Manna, S.; Chowdhury, S. R.; Sen, R.; Roy, D.; Adhikari, B. *Bioresour. Technol.* **2010**, *101*, 3182.
- Adrian, J. N.; Jose, M. K.; Maria, M. R.; Mirta, I. A.; Norma, E. M. *Polym. Eng. Sci.* **2002**, *42*, 732.
- Joseph, P. V.; Joseph, K.; Thomas Pillai C. K. S.; Prasad, V. S. Groeninckx, G.; Sarkissova, M. *Compos. Part A Appl. Sci. Eng.* **2003**, *34*, 253.
- Fardausy, A.; Kabir, M. A.; Kabir, H.; Rahman, M. M.; Begum, K.; Ahmed, F.; Hossain, M. A.; Gafur, M. A. *Int. J. Adv. Res. Eng. Technol.* **2012**, *3*, 267.
- Mohanty, S.; Nayak, S. K. *J. Appl. Polym. Sci.* **2006**, *102*, 3306.
- Fuad, M. Y. Mustafah, J.; Mandor, M. S.; Mohd Ishak, Z. A.; Mohd Omar, A. K. *Polym. Intl.* **1995**, *38*, 33.
- Gann, R. G.; Dipert, A.; Drews, M. J. In *Encyclopedia of Polymer Science and Engineering*, 2nd ed.; Kroschwitz, J. I., Ed.; Wiley: New York, **1987**; Vol.7, pp 154.
- Beall, F. C. In *Encyclopedia of Polymer Science and Engineering*; Bever, M. B., Ed.; Pergamon Press: Oxford, **1986**; Vol.7.
- Kumer, R. V.; Koltypin, Y.; Gedanken, A. *J. Appl. Polym. Sci.* **2002**, *86*, 160.